Investigation of Miniaturized Radioisotope Thermionic Power Generation for General Use

Adam J. Duzik*[a] and Sang H. Choi[b]
[a]National Institute of Aerospace, 100 Exploration Way, Hampton, VA, 23666;
[b]NASA Langley Research Center, 8 West Taylor St., Hampton, VA, 23681

ABSTRACT

Radioisotope thermoelectric generators (RTGs) running off the radioisotope Pu^{238} are the current standard in deep space probe power supplies. While reliable, these generators are very inefficient, operating at only ~7% efficiency. As an alternative, more efficient radioisotope thermionic emission generators (RTIGs) are being explored. Like RTGs, current RTIGs concepts use exotic materials for the emitter, limiting applicability to space and other niche applications. The high demand for long-lasting mobile power sources would be satisfied if RTIGs could be produced inexpensively. This work focuses on exposing several common materials, such as Al, stainless steel, W, Si, and Cu, to elevated temperatures under vacuum to determine the efficiency of each material as inexpensive replacements for thermoelectric materials.

Keywords: Radioisotope thermoelectric generators, thermionic generator, thermionic emission

1. INTRODUCTION

Small, portable, low-power consumption devices continue to increase in usage, often supplanting older devices requiring more power. Smartphones and tablets are quickly replacing laptops in portable computing,[1] driving an ever-increasing demand for longer run-times without recharging. This has not only driven the development of high-performance, low power consumption processors, but has pushed current Li battery technology to thinner form factors and higher power densities. Despite these advancements, the need for recharging cannot be eliminated entirely, only postponed. Current wireless charging technology relies on close proximity and is effectively no better than wired methods in this respect. Recharging via portable solar cells is another possibility, but is of limited usefulness at night or inside buildings.

An alternative to this paradigm is to adapt a well-established technology used in deep space probe applications. The radioisotope thermoelectric generator (RTG) is the current power source for probes such as *Pioneer*,[2] *Voyager*,[3] *Cassini*, and *New Horizons*,[4] providing consistent power for several decades. The RTG "fuel" is a few kilograms of Pu^{238}, a radioactive isotope with a half-life of about 87 years. Pu^{238} decays at ~1000°C, generating about 0.55 W/g of thermal power.[5] A thermoelectric device then converts that thermal energy into usable electrical power. Current RTG efficiency is about 7%, which forces the use of larger generators and more Pu^{238} to achieve a usable amount of power.

Thermionic emission has been proposed as an alternative mechanism for converting thermal energy to electrical power. Thermoelectric generators must obey the figure of merit equation, which requires high electrical conductivity and low thermal conductivity in the p- and n- doped semiconductors, two properties that rarely coexist in one material. Instead, a thermionic emitter has the best thermal insulator (vacuum) and can emit electrons unrestricted by a material mobility. Estimates have put thermionic engine efficiency at values of over 20%.[6]

Most research on thermionic engines has focused on exotic materials, such as LaB_6 doped diamond.[7–10] This is impractical for mass production of economical thermionic engines. As such, this work focuses on the use of more common materials, such as Cu, stainless steel, Al, Ta, W, n-Si wafers, and SiGe/Sapphire thin films as alternative, low-cost emitters. While these may not be as efficient as traditional emitters such as LaB_6 or more exotic emitters such as doped diamond, they do not need to be for most low power consumption mobile devices. Current smartphones and tablets run on the order of 10-15W or less,[11–13] requiring only a small amount of material to produce the necessary power and still fit into current battery weights and dimensions.

*adam.j.duzik@nasa.gov; phone 1 757-864-6030

2. EXPERIMENTAL SETUP

All thermionic emission experiments were performed in a vacuum chamber. The side view of the sample holder, stage, and collector plates are shown in Figure 1. Each sample was clamped into the Cu bracket, positioned so the emission surface in each run was the same distance from the collector plate. W and Ta samples were short wires, approximately 25 mm in length. All other sample emission surfaces were either flat or pointed, produced from large sheets of material. Flat samples were simply cut out of the larger material stock and loaded into the Cu bracket. The pointed emission samples were produced by drilling two holes such that the edges touch, resulting in the samples shown in Figure 2. This creates a sharp cusp at the emission surface. Separate runs for a gap distance of 3mm and 1mm were performed for the pointed samples, while all flat end samples were run with a 3mm gap.

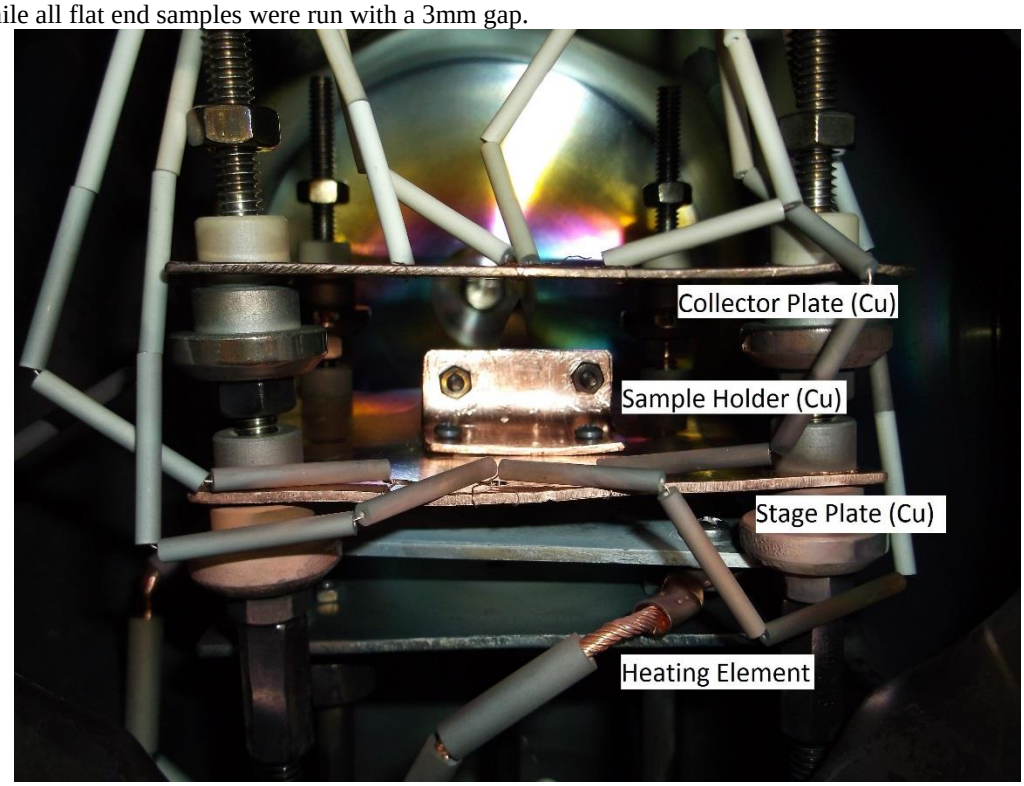

Figure 1. Thermionic emission test setup

Emission current was measured with a picoammeter connected to the collector plate through an electrical feed through as shown in Figure 3. A small power supply was wired in series with the picoammeter, taking the common output from it into the positive terminal on the power supply, with the negative lead connected to the stage plate. This allowed application of a 0-18V bias voltage to see the effects on emission for each material. Finally, the space charge effects were also measured during the runs. The vacuum chamber used both a turbomolecular pump and an ion pump. Turning off the ion pump resulted in a sudden pressure increase, and the subsequent decrease in emission current was recorded.. In other work, cesium-based atmospheres showed decreased space charge barrier effects and improved emission efficiency. However, all of these measurements were carried out under vacuum, as this will be a more likely scenario in a commercial device.[14–16]

Figure 2. Samples used for thermionic emission. Top side of each shows the pointed end, the bottom side the square ends. The W wire on the right was for reference purposes.

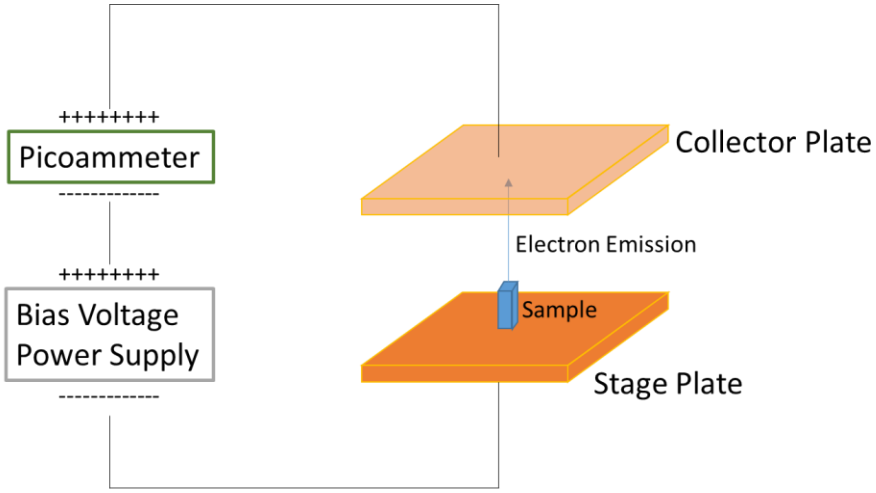

Figure 3. Circuit diagram of thermionic emission setup.

3. EXPERIMENTAL RESULTS

The emission current vs. temperature data are plotted in Figure 4. The emission current was normalized with sample thickness or wire diameter; hence the units are current/unit length. In Figure 4a, the emission currents are on the order of 100 nA/mm for most samples upon sufficient heating to produce thermionic emission. Ta wire shows the highest response, reaching 1 uA above 450°C. Stainless steel also produced a strong response, reaching 700 nA/mm at 500°C. The semiconductors of n-type Si (n-Si) and SiGe/Al_2O_3 showed an emission current above 700°C, but only to 500 nA/mm and 600 nA/mm, respectively. Cu showed a small response, only producing 200 nA/mm above 600°C. In Figure 4b, the square end samples did not show much response for any material. The Ta and W wire reference samples produced as much or more current than most of the pointed or flat samples despite the wires having less emission surface area. Unfortunately, these results suggest that pointed emitters must be used to obtain a usable current instead of the flat, square emitters more conducive to power cell construction. Fortunately, shorter gap distances produced much better results. In Figure 4c, the pointed emitters were tested with a 1mm gap distance vs. the 3mm gap distance in Figure 4a. Cu shows a much bigger response, reaching a peak emission current of 9 μA/mm. The next closest sample was Ta wire, at 2 μA/mm. Stainless steel, the better emitter at 3mm, showed a similar emission current at a 1mm gap and almost two orders of magnitude less than Cu emission. These results point to Cu as the material of choice.

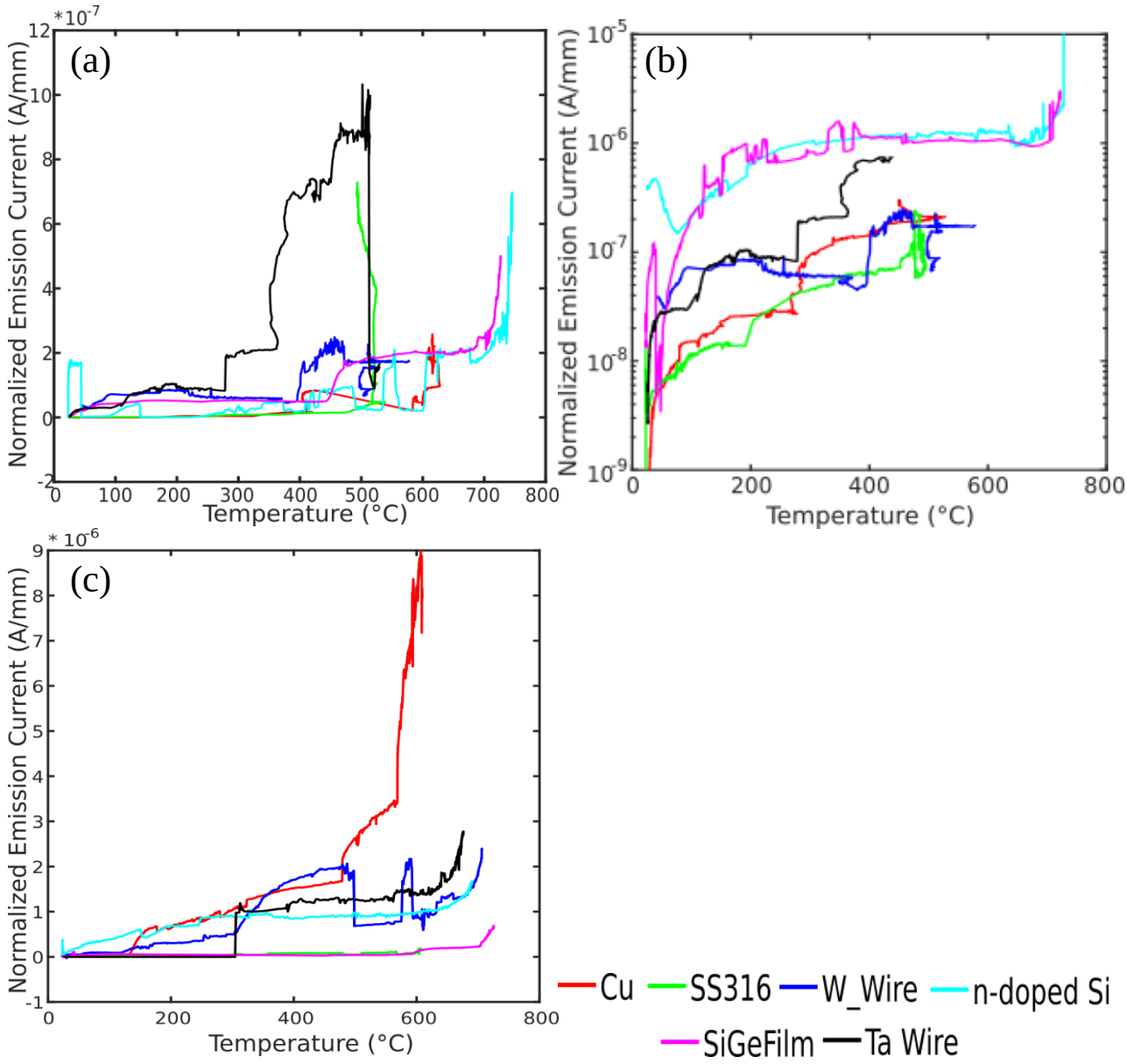

Figure 4. Emission vs. temperature for the six pointed samples at (a) a 3mm gap distance, (b) a 1mm gap distance, and (c) square samples at a 3mm gap distance. (a) and (c) are in linear scale, (b) is in log scale.

The decrease in emission current due to increased space charge is plotted in Figure 5. Solid lines represent the emission current, measured on the left axis, and the dashed lines represent the pressure, measured on the right axis. Also, these measurements were taken after the temperature had stabilized for a long time (at least 30 minutes). In this time, some of the sample emission currents became unstable, rising or falling from the peak values in Figure 4. For the 3mm gap results of the pointed end samples in Figure 5a, n-doped Si and stainless steel showed a decrease in emission current of 0.133 A/torr and 0.166 A/torr, respectively. Cu and W wire showed low responses to increased pressure, only 0.022 A/torr and 0.015 A/torr while Ta wire appeared invariant with pressure. Given the low emission currents these materials were already exhibiting, this is unsurprising. The square ended emission surfaces of Figure 5b show similar results, with Cu showing a lower sensitivity to increased pressure over stainless steel. Finally, the 1mm gap results are shown in Figure 5c. Both the semiconductor samples show little overall change after the pressure jump; SiGe shows a momentary decrease, but then returns to its original value. All the metallic samples except for W showed no change in current with pressure, indicating emission current saturation. W showed a change of 0.812 A/torr-mm. While Cu still has a large potential current, W seems

to be more stable with temperature. The deciding factor between the two is how effective a bias voltage is in extracting more current.

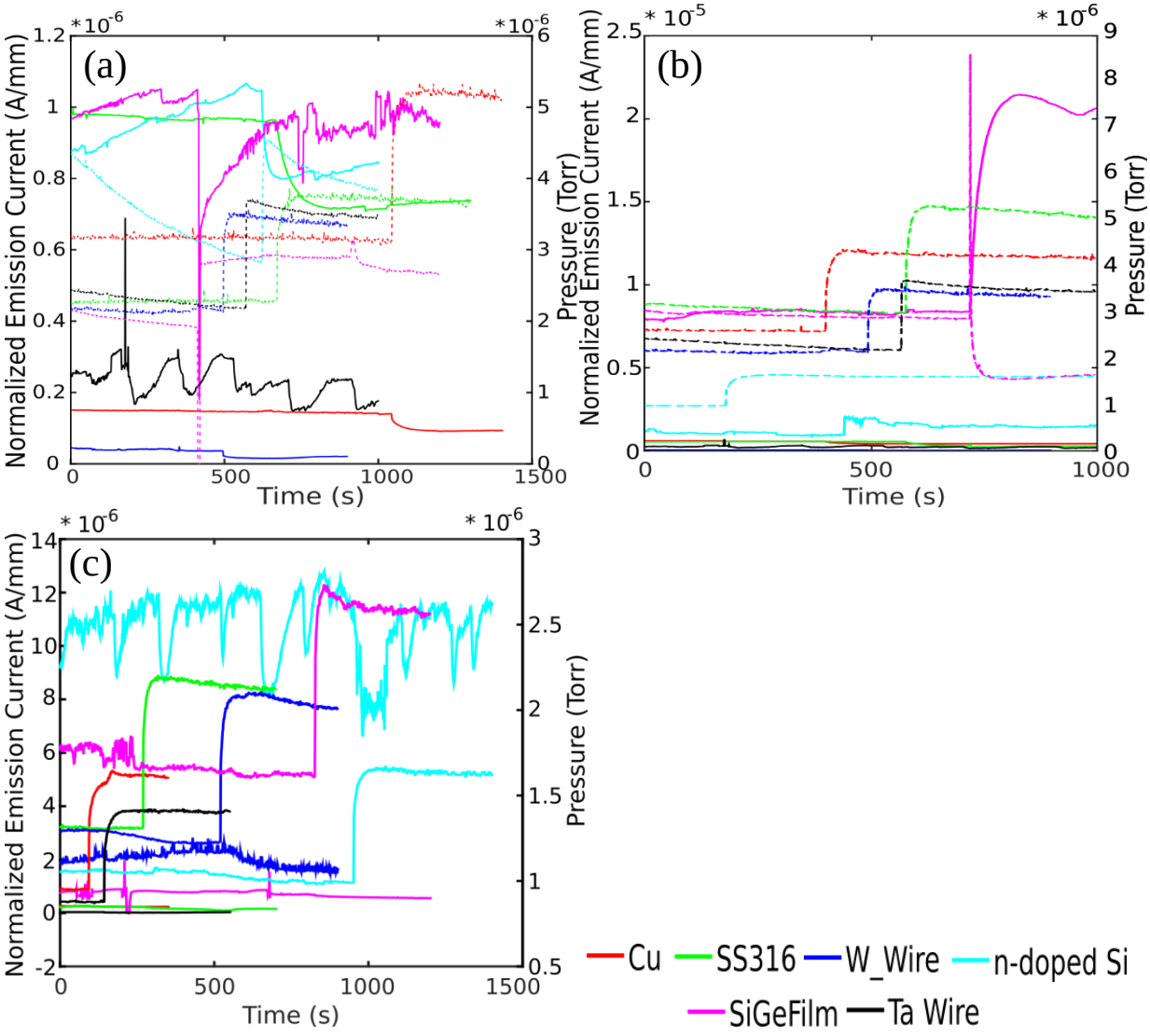

Figure 5. Emission current and pressure change before and after the ion pump was turned off.

Changes in emission current vs. applied bias voltage are plotted in Figure 6. All emission current data points for a given sample were normalized with respect to the emission current obtained at 0V (no bias); the increase or decrease in current is a multiplier of the unbiased value. In Figure 6a and b, the pointed and square emission surfaces were tested at the 3mm gap distance, with similar results. Most samples respond to the bias voltage increase in a somewhat linear fashion, increasing by a certain amount for each additional volt, regardless of emission surface shape. For some samples, such as the W wire and the stainless steel flat end, the multiplier was rather erratic, showing large jumps between voltage increments. This is explained as oscillation from low signal to noise ratio, that is, the emission current was at a low level (200 nA/mm or less) and thus less discernable from electronic signal and thermal noise in the measurement. In the case of the Cu pointed emitter, a small decrease was observed, which remained largely consistent even with more applied bias.
At a 1mm gap, the behavior changes. Cu shows the strongest response, the emission current increasing tenfold at 18V, while other samples tend to saturate or even decrease with increasing voltage. From this, it is concluded all samples but Cu have reached maximum emission at the 1mm gap distance; increasing the bias voltage makes the emission of electrons across the gap more favorable, but the lack of electrons limits the benefit seen. On the other hand, Cu clearly shows no

saturation. This can be attributed to Cu having the highest electrical conductivity of any material tested here, resulting in a much higher threshold for saturation.

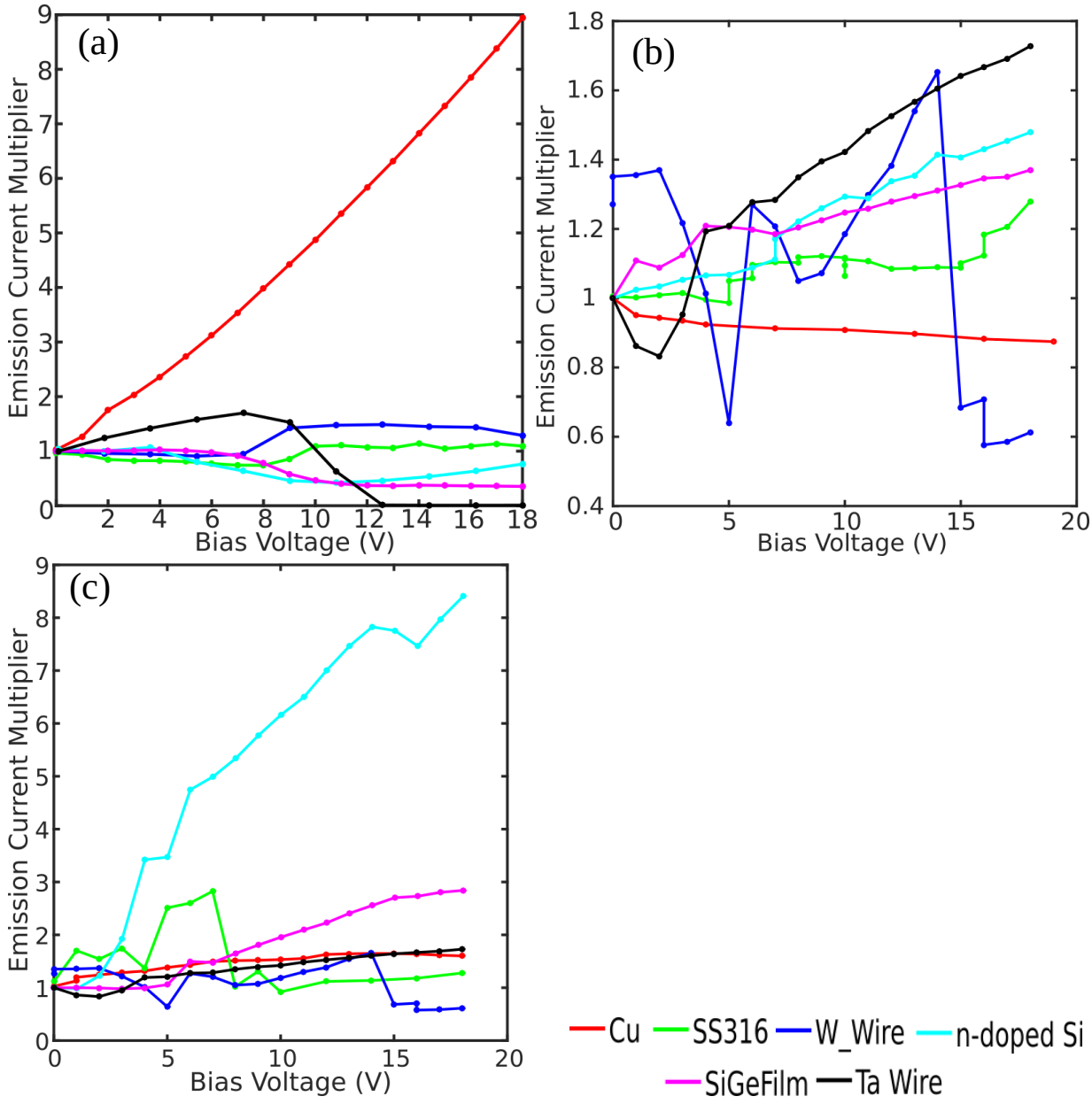

Figure 6. Emission current multiplier vs. applied bias voltage

4. PROPOSED CELL DESIGN

Based on the above results, a small, compact power source is proposed as a replacement for batteries in low consumption devices. As such, the cell needs to satisfy a number of conditions:

4.1 Output 10-15W of power

The above results show Cu emission reaches $9*10^{-6}$ A/mm at its peak, and for a copper work function of 4.7eV, a single electron reaches the collector at 4.6V with no bias voltage, giving ~$4*10^{-5}$ W/mm of ridge length.[17] This is encouraging,

as 10^5 mm or 100 m of Cu will produce enough emission to generate 4 W of continuous power. Modern semiconductor processing uses Cu as via channel material, with device sizes reducing to 10 nm and less. As such, pointed ridges could be produced with only a 10 nm gap between them, or 10^5 ridges in 1 mm. If each ridge is 1mm long, then a 1mm x 1mm space could theoretically produce 4 W of current. Realistically, the ridges will need to be further spaced, likely 1um apart or more, in order to prevent electron emission between ridges. This requires 100 times the area, or 1 cm^2, still well within the desired form factor. At most, a 4 cm^2 active region will supply 16 W of power, enough for many devices.

The next question is how much Pu^{238} is necessary to maintain emission. Current technology permits the use of thin vacuum insulation around any shape, ideal for this application. A cell 2x2x0.5 cm^3 in size with a 0.5 mm vacuum layer will lose only 1.8 W of thermal power, assuming a vacuum thermal conductivity of 0.001 W/m·K. Pu^{238} yields 0.57 W/g of thermal power, meaning a cell would require ~ 3 g of Pu^{238}. At a 1 mm vacuum thickness, only 1.5 g are required to maintain emission.

Finally, the collector plate must be closer to the point of the ridges than the spacing between ridges, also to prevent transmission between ridges and to increase the emission current. Scanning tunneling microscopy (STM) routinely achieves gap distances of 1 nm or less using piezoelectric actuators; such methods could position the collector to within a small gap, maintained by supports to the active material in the center of the cell. Even with some current used to maintain a constant bias voltage, the necessary power requirements can be met in such a compact size.

4.2 Achieve necessary power output under vacuum

These materials were tested in a vacuum environment of 10^{-6} torr or less to simulate the conditions within a sealed device. Efforts focused on cesium (Cs) vapor thermionic converters show less space charge and higher efficiency, but cost, safety, and environmental concerns are all potential issues.[14–16] Therefore, the proposed design does not rely on Cs vapor as an option; it must achieve realistic power output with vacuum only. If a cost-effective, safe utilization of Cs into a cell is realized, then the proposed device will operate at a higher efficiency.

4.3 Maintain a high thermal gradient while protecting the user

Such levels of current require internal cell temperature to be maintained at approximately 700°C at all times. To maintain the small shape factor, a strong insulator is required. Recent advances in vacuum cavity insulation provide the solution, and can be molded to any shape to produce a 1mm vacuum gap of thermal insulation around any part, enough to maintain the 700°C temperature inside and room temperature outside while maintaining the desired slim form-factor.

4.4 Protect against radiation

The last design consideration is important from a safety standpoint. Pu^{238} is primarily an alpha-emitter, with a small level of gamma-radiation, and requires only a small amount of lead shielding, around 2.5mm.[5] As such, it has been used successfully in pacemakers,[18,19] proving Pu^{238} has a strong safety record. Given this low shielding requirement, Pu^{238} is the only isotope known to provide enough heat while fitting into the small form factor of a battery.

5. CONCLUSION

Several thermionic emission sample materials were tested to find an emitter material for use in a mass production power cell as a replacement for batteries in low-power electronics. The pointed copper ridge sample proved to be the most promising emitter, producing $9*10^{-6}$ A/mm when placed at a 1 mm gap from the collector plate. Cu also showed a lower sensitivity to space charge buildup, a necessary requirement for sustained use. A continuous power cell design was proposed, wherein modern semiconductor patterning and etching techniques can be used to create a micron-scale or smaller series of Cu ridges positioned less than a micron from a collector plate, with the potential to generate a significant amount of power in a small form factor suitable for mobile devices.

REFERENCES

[1] Frommer, D., “Smartphone sales to beat PC sales by 2011,” Bus. Insid., 2009, <http://www.businessinsider.com/chart-of-the-day-smartphone-sales-to-beat-pc-sales-by-2011-2009-8> (3 February 2016).

[2] Skrabek, E. A.., McGrew, J. W., “Pioneer 10 and 11 RTG performance update,” Sp. Nucl. Power Syst., 201–204 (1987).

[3] De Winter, F., Stapfer, G.., Medina, E., "Design of a nuclear power supply with a 50 year life expectancy: the JPL Voyager's SiGe MHW RTG," IEEE Aerosp. Electron. Syst. Mag. **15**(4), 5–12 (2000).
[4] Bennett, G. L., Lombardo, J. J., Hemler, R. J., Silverman, G., Whitmore, C. W., Amos, W. R., Johnson, E. W., Zocher, R. W., Hagan, J. C., et al., "The general-purpose heat source radioisotope thermoelectric generator: A truly general-purpose space RTG," AIP Conf. Proc. **969**, 663–671 (2008).
[5] Arnold, E. D., Handbook of Shielding Requirements and Radiation Characteristics of Isotopic Power Sources for Terrestrial, Marine, and Space Applications, Clearinghouse for Federal Scientific and Technical Information, Springfield, VA (1964).
[6] Ryan Smith, J., "Increasing the efficiency of a thermionic engine using a negative electron affinity collector," J. Appl. Phys. **114**(16), 164514 (2013).
[7] Futamoto, M., Nakazawa, M.., Kawabe, U., "Thermionic Emission Properties of Hexaborides," Surf. Sci. **100**, 470–480 (1980).
[8] Olsen, G. H.., Cafiero, A. V., "Single-crystal growth of mixed (La, Eu, Y, Ce, Ba, Cs) hexaborides for thermionic emission," J. Cryst. Growth **44**(3), 287–290 (1978).
[9] Koeck, F. A. M., Nemanich, R. J., Balasubramaniam, Y., Haenen, K.., Sharp, J., "Enhanced thermionic energy conversion and thermionic emission from doped diamond films through methane exposure," Diam. Relat. Mater. **20**(8), 1229–1233 (2011).
[10] Kataoka, M., Zhu, C., Koeck, F. A. M.., Nemanich, R. J., "Thermionic electron emission from nitrogen-doped homoepitaxial diamond," Diam. Relat. Mater. **19**(2-3), 110–113 (2010).
[11] Wang, W., "An Analysis of Power Consumption in a Smartphone Wei Wang," <http://web.cs.wpi.edu/~emmanuel/courses/cs525m/S13/slides/smartphone_power_analysis_wei_wang_wk9.pdf > (12 January 2016).
[12] Apple, I., "iPad Air 2 Technical Specifications," <http://www.apple.com/ipad-air-2/specs/> (12 January 2016).
[13] Carroll, A.., Heiser, G., "An analysis of power consumption in a smartphone," Proc. 2010 USENIX Conf. USENIX Annu. Tech. Conf., 21–21 (2010).
[14] Rasor, N. S., "The Cesium Vapor Thermionic Converter. I. Limitations Imposed by Emission Processes," Advan. Energy Convers. **2** (1962).
[15] Rasor, N. S., "Experimental Research on the Cesium Thermionic Converter," IAS 29th Annu. Meet. New York (January 1961) (1961).
[16] Rasor, N. S. S., "Emission physics of the thermionic energy converter," Proc. IEEE **51**(5), 733–747 (1963).
[17] E. W. J. Mitchell, J. W. M., "The Work Functions of Copper, Silver and Aluminium," Proc. R. Soc. Lond. A. Math. Phys. Sci. **210**(1100), 70–84, The Royal Society (1951).
[18] Huffman, F. N., Migliore, J. J., Robinson, W. J.., Norman, J. C., "Radioisotope Powered Cardiac Pacemakers," Cardiovasc. Dis. **1**, 52–60 (1974).
[19] Parsonnet, V., Driller, J., Cook, D.., Rizvi, S. A., "Thirty-one years of clinical experience with nuclear-powered pacemakers," PACE - Pacing Clin. Electrophysiol. **29**(2), 195–200 (2006).